Influence of the upper waveguide layer thickness on optical field in asymmetric heterostructure quantum well laser diode

Peixu Li (李沛旭)[1,2], Kai Jiang (蒋 锴)[1,2], Shuqiang Li (李树强)[1,2], Wei Xia (夏 伟)[1,2], Xin Zhang (张 新)[2], Qingmin Tang (汤庆敏)[2], Zhongxiang Ren (任忠祥)[2], and Xiangang Xu (徐现刚)[1,2*]

[1]*State Key Laboratory of Crystal Material, Shandong University, Ji'nan 250100, China*

[2]*Shandong Huaguang Optoelectronics Co., Ltd., Ji'nan 250101, China*

[*]*E-mail: xxu@sdu.edu.cn*

Received September 17, 2009

Asymmetric broad-waveguide separate-confinement heterostructure (BW-SCH) quantum well (QW) laser diode emitting at 808 nm is analyzed and designed theoretically. The dependence of the optical field distribution, vertical far-field angle, and internal loss on different thicknesses of the upper waveguide layer is calculated and analyzed. Calculated results show that when the thicknesses of the lower and upper waveguide layers are 0.45 and 0.3 μm, respectively, for the devices with 100-μm-wide stripe and 1000-μm-long cavity, an output power of 7.6 W at 8 A, a vertical far-field angle of 37°, a slope efficiency of 1.32 W/A, and a threshold current of 189 mA can be obtained.

OCIS codes: 140.2020, 140.5960, 230.5590.

doi: 10.3788/COL20100805.0493.

Semiconductor lasers emitting at a wavelength of 808 nm have been developed for approximately two decades. However, interests in these lasers have not decreased, since they are widely used in systems for pumping solid-state lasers and in fiber optics amplifiers thanks to the main advantages of these lasers[1−3]. Rapid development of the electronic industry requires continual improvement of laser diodes (LDs), such as the performance of optical power, radiation intensity, efficiency, and operation life.

In order to improve the characteristics of 808-nm quantum well (QW) LDs, various approaches are used. Now, the most widely used structure is broad-waveguide separate confinement heterostructure (BW-SCH) or the structure with a super-large optical cavity[4−7]. These structures have a large equivalent transverse spot size d/Γ, where d is the active layer thickness and Γ is the optical confinement factor. It is highly desirable to increase the value of catastrophic optical mirror damage (COMD). Thus the purpose of increasing the maximum output power of the diode laser will be achieved. However, the improvement of the d/Γ value by lowering the optical confinement factor is limited because of the injected-carrier leakage and higher optical mode. In those symmetric structures, it is also subject to mode instabilities due to the weak mode confinement and thermal lens[8]. In particular, it has been shown recently that the use of an asymmetric heterostructure in an AlGaAs/GaAs or AlGaInP/GaInP system makes it possible to appreciably reduce the internal optical losses and increase the maximum optical power[9−14].

In this letter, the effect of the thickness on the upper waveguide layer in the asymmetric heterostructure in InGaAsP/GaInP/AlGaInP system is studied. The dependence of the optical field distribution, the vertical far-field angle, and the internal loss on the thickness of the upper waveguide layer is calculated and analyzed. Meanwhile, LDs are produced and tested with the structures.

In order to analyze the characteristics of the optical field, the waveguide structure is taken as one-dimensional (1D) broad waveguide structure. For TE mode, the wave function is

$$\frac{\mathrm{d}^2u(x)}{\mathrm{d}x^2} + [k_0^2n^2(x) - \beta^2]u(x) = 0, \tag{1}$$

where $k_0 = \frac{2\pi}{\lambda}$ is the wave number, $n(x)$ is the index, β is the propagation constant. By the boundary condition of the TE mode, the wave function $u(x)$ can be calculated. The optical confined factor Γ can be obtained by using $u(x)$:

$$\Gamma = \int_{\text{active}} u^2(x)\mathrm{d}x \Big/ \int_{\text{all}} u^2(x)\mathrm{d}x, \tag{2}$$

where $\int_{\text{active}}$ and $\int_{\text{all}}$ are the integral of the active region and the whole optical field distribution region. Then the equivalent transverse spot size d/Γ can also be obtained. The intensity of the optical field is

$$\frac{I(\theta)}{I(0)} = \cos^2\theta \left| \int_{\text{all}} u(x)\exp[\mathrm{i}(k_0\sin\theta)x]\mathrm{d}x \right|^2 \Big/ \left| \int_{\text{all}} u(x)\mathrm{d}x \right|^2. \tag{3}$$

When $\frac{I(\theta)}{I(0)} = \frac{1}{2}$, the angle $\theta_{1/2}$ equals half of the vertical far-field angle $\theta_\perp$, then $\theta_\perp$ is

$$\theta_\perp = 2\theta_{1/2}. \tag{4}$$

The optical absorption out of the active layer is proportional to the doped consistency. The asymmetric BW structure is designed based on the fact that the optical absorption in n-type semiconductor materials is lower than that in p-type semiconductor materials. The structure investigated in this study consisted of p-doped $(Al_{0.4}Ga_{0.6})_{0.52}In_{0.48}P$ and n-doped $(Al_{0.2}Ga_{0.8})_{0.52}In_{0.48}P$ asymmetric cladding layers, which was beneficial for reducing the optical absorption in the active region. Three cases of the upper

waveguide layer thickness of 150, 300, and 450 nm were chosen to analyze the effect.

All the asymmetric BW laser structures were grown by low-pressure metal organic chemical vapor deposition (MOCVD). The source materials were trimethylindium, trimethylgallium, and trimethylaluminum for the group III elements; arsine and phosphine for the group V elements; diethylzinc, silane diluted to 0.02% in hydrogen for the dopants. Palladium-diffused hydrogen was used as the carrier gas. One 8-nm-thick InGaAsP QW surrounded by the $Ga_{0.52}In_{0.48}P$ waveguide layer was located close to the 1.0-μm-thick p-doped $(Al_{0.4}Ga_{0.6})_{0.52}In_{0.48}P$ cladding layer. The lower waveguide thickness was 0.45 μm while the thickness of upper waveguide was 0.15, 0.3, and 0.45 μm corresponding to the structures a, b, and c, respectively. 1.0-μm-thick $(Al_{0.2}Ga_{0.8})_{0.52}In_{0.48}P$ was used as the n-cladding layer.

Also, the symmetric BW laser structure was grown by LP-MOCVD. In the structure we used 1.0-μm-thick $(Al_{0.4}Ga_{0.6})_{0.5}$ $In_{0.5}P$ as the cladding layers and 0.45-μm-thick GaInP as the waveguide layers.

Broad area lasers with 100-μm-wide stripe were fabricated. The LDs were coated with 15% antireflection (AR) coating on the front facet and 95% high-reflection (HR) coating on the rear facet and were bonded with a p-side down configuration on the Cu heatsink.

Figure 1 shows the calculated optical field distribution in the asymmetric structures. The thick plumb lines stands for the location of the QW, and others stand for the locations of the interfaces between the upper waveguide layer and the p-doped cladding layer. It shows that with the thickness of the upper waveguide layer reducing, the peak optical intensity is pushed away from the QW, which will be beneficial for reducing the optical absorption of the injected free carriers. In these asymmetric structures, the optical field is prevented from penetrating into the p-cladding layer. But in structure a, perhaps the thickness of the upper waveguide layer is so small that the optical field penetrates into p-cladding layer more deeply than other structures.

Figure 2 shows the relationship between the thickness of the upper waveguide layer and the vertical far-field angle $\theta_\perp$. This angle reduces with the increase of the upper waveguide layer thickness. It decreases from 39° at 0.15 μm to 35° at 0.45 μm. The angle $\theta_\perp$ does not vary largely due to the small changes of the upper waveguide layer thickness.

The internal loss α_i of the laser is calculated using the

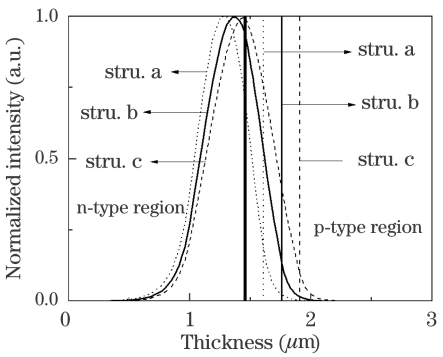

Fig. 1. Calculated optical field distribution in the asymmetric structures.

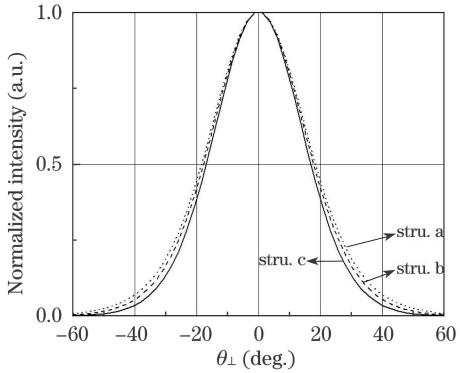

Fig. 2. Vertical far-field angle of different structures.

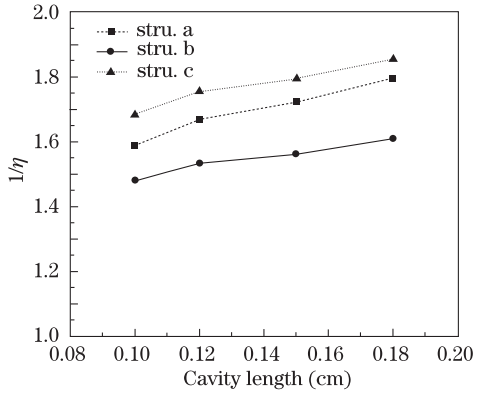

Fig. 3. Reciprocal external differential quantum efficiency as a function of cavity length.

cavity length and the differential quantum efficiency as

$$\frac{1}{\eta_d} = \frac{1}{\eta_i}\left(1 + \alpha_i \frac{1}{\frac{1}{2L}\ln\frac{1}{R_1 R_2}}\right), \tag{5}$$

where η_d and η_i are the differential quantum efficiency and the injection efficiency, L is the cavity length, R_1 and R_2 are the reflectivity of the front and back facets, respectively.

The power-current characteristics of devices with varying cavity lengths L are measured under continuous wave (CW) condition at room temperature. The internal loss α_i of the structures a, b, and c are 4.8, 2.7, and 3.5 cm^{-1}, respectively. In structure a, the optical field penetrates into p-cladding layer more deeply than others which brings in more absorption. Meanwhile, the interface of the waveguide layer and cladding layer is nearer to the QW which also brings in more absorption. The result is shown in Fig. 3.

The influences of the design variations on the electro-optical laser parameters are studied on uncoated devices with a stripe width of 100 μm under CW condition at room temperature. The experimental results are compiled in Table 1. The vertical far-field angle $\theta_\perp$ at full-width at half-maximum (FWHM), threshold current I_{th}, and slope efficiency S are given for 1-mm-long devices.

From the results, the LD is superior if the thickness of the upper waveguide layer is optimized. In the experiment, structure b is the best. With structure b, the power-current and efficiency-current characteristics of 1-mm-long lasers with stripe width of 100 μm are shown in Fig. 4(a). Figure 4(b) shows the CW output power and

Table 1. Compilation of Data Obtained from Devices Without Coating. The Stripe Width is 100 μm

L=1 mm				
Structure	$\theta(^\circ)$	$I_{\rm th}$(mA)	$E_{\rm s}$(W/A)	$\alpha_{\rm i}$(cm^{-1})
a	39	295	0.62	4.8
b	37	235	0.68	2.7
c	35	196	0.6	3.5

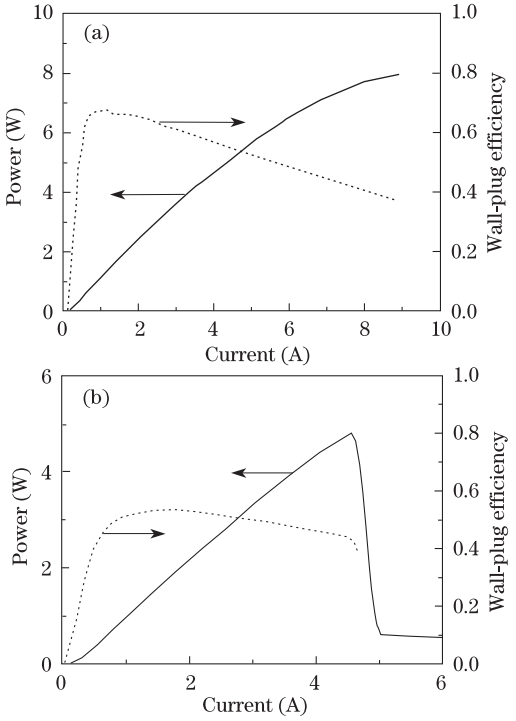

Fig. 4. CW output power and wall-plug efficiency at room temperature of (a) structure b and (b) symmetric BW LD.

wall-plug efficiency of symmetric BW LD at room temperature. From Fig. 4(a), it can be seen that the 100-μm-stripe-width device achieves the maximum output power of more than 7.6 W at an injection current of 8 A limited by thermal rollover. A threshold current $I_{\rm th}$ of 189 mA and a slope efficiency $E_{\rm s}$ of 1.32 W/A are obtained. The maximum conversion efficiency is more than 60%.

In conclusion, the thickness of the upper waveguide layer in the asymmetric BW-SCH QW laser has a great effect on the optical field, vertical far-field angle, and internal loss. The dependence of the optical field distribution, vertical far-field angle, and internal loss on the thickness of the upper waveguide layer is analyzed and calculated. With the optimized structures, LDs are produced and tested under CW condition at room temperature. The experiment demonstrates 7.6-W CW optical power at an injection current of 8 A. Meanwhile, a threshold current $I_{\rm th}$ of 189 mA, a vertical far-field angle of 37°, a slope efficiency of 1.32 W/A, and a maximum conversion efficiency of more than 60% are obtained from a 100-μm-wide stripe and 1000-μm-long cavity device.

This work was supported by the National Natural Science Foundation of China (No. 50472068) and the Program for New Century Excellent Talents in University.

References

1. Y. Qu, S. Yuan, C. Liu, B. Bo, G. Liu, and H. Jiang, IEEE Photon. Technol. Lett. **16,** 389 (2004).
2. R. K. Huang, B. Chann, L. J. Missaggia, J. P. Donnelly, H. T. Harris, G. W. Turner, A. K. Goyal, T. Y. Fan, and A. Sanchez-Rubio, IEEE Photon. Technol. Lett. **19,** 209 (2007).
3. G. Fang, J. Xiao, X. Ma, X. Feng, X. Wang, Y. Liu, B. Liu, M. Tan, and Y. Lan, Chin. J. Semicond. (in Chinese) **23,** 809 (2002).
4. J. K. Wade, L. J. Mawst, D. Botez, and J. A. Morris, Electron. Lett. **34,** 1100 (1998).
5. F. Dittmar, B. Sumpf, J. Fricke, G. Erbert, and G. Trankle, IEEE Photon. Technol. Lett. **18,** 601 (2006).
6. A. Knauer, G. Erbert, R. Staske, B. Sumpf, H. Wenzel, and M. Weyers, Semicond. Sci. Technol. **20,** 621 (2005).
7. J. Li, J. Han, J. Deng, D. Zou, and G. Shen, Chinese J. Lasers (in Chinese) **33,** 1159 (2006).
8. M. Buda, W. C. van der Vleuten, G. Iordache, G. A. Acket, T. G. van der Roer, C. M. van Es, B. H. van Roy, and E. Smalbrugge, IEEE Photon. Technol. Lett. **11,** 161 (1999).
9. K. Shigihara, K. Kawasaki, Y. Yoshida, S. Yamamura, T. Yagi, and E. Omura, IEEE J. Quantum Electron. **38,** 1081 (2002).
10. J. J. Lee, L. J. Mawst, and D. Botez, J. Cryst. Growth **249,** 100 (2003).
11. V. V. Bezotosnyi, V. V. Vasil'eva, D. A. Vinokurov, V. A. Kapitonov, O. N. Krokhin, A. Yu. Leshko, A. V. Lyutetskii, A. V. Murashova, T. A. Nalet, D. N. Nikolaev, N. A. Pikhtin, Yu. M. Popov, S. O. Slipchenko, A. L. Stankevich, N. V. Fetisova, V. V. Shamakhov, and I. S. Tarasov, Semiconductors **42,** 350 (2008).
12. N. A. Pikhtin, S. O. Slipchenko, Z. N. Sokolova, A. L. Stankevich, D. A. Vinokurov, I. S. Tarasov, and Z. I. Alferov, Electron. Lett. **40,** 1413 (2004).
13. L. Lin, G. Liu, Z. Li, M. Li, X. Wang, H. Li, and H. Tan, Chin. Opt. Lett. **6,** 268 (2008).
14. P. Li, L. Wang, S. Li, W. Xia, W. Zhang, Q. Tang, Z. Ren, and X. Xu, Chin. Opt. Lett. **7,** 489 (2009).